

Elements of a theory for the mechanisms controlling abundance, diversity, and biogeochemical role of lytic bacterial viruses in aquatic systems

T. Frede Thingstad

Department of Microbiology, University of Bergen, Jahnebakken 5, N-5020 Bergen, Norway

Abstract

Mechanisms controlling virus abundance and partitioning of loss of bacterial production between viral lysis and protozoan predation are discussed within the framework of an idealized Lotka-Volterra-type model. This combines nonselective protozoan predation with host-selective viral lysis of bacteria. The analysis leads to a reciprocal relationship between bacterial diversity and viruses, in which coexistence of competing bacterial species is ensured by the presence of viruses that “kill the winner,” whereas the differences in substrate affinity between the coexisting bacterial species determine viral abundance. The ability of the model to reproduce published observations, such as an approximate 1:10 ratio between bacterial and viral abundance, and the ability of viral lysis to account for 10–50% of bacterial loss are discussed.

Viral abundance in aquatic environments can now be determined by different techniques, such as centrifugation combined with electron microscopy (Bergh et al. 1989; Proctor and Fuhrman 1990), fluorescence microscopy (Noble and Fuhrman 1998), and, at least in cultures, by flow cytometry (Brussaard et al. 1999). Indications are that natural abundances of viruses are typically on the order of 10^{10} L⁻¹ but range from 3×10^8 to 1×10^{11} L⁻¹ (Fuhrman 1999; Wilhelm and Suttle 1999). Most of these viruses have been assumed to have bacteria as their host organisms (Bratbak et al. 1994). Measurements of decay rates vary, but they seem to provide numbers on the order of 0.05–1.1 h⁻¹ (Heldal and Bratbak 1991). Combined with a detectable infection frequency of around 2–24% of the host population (Heldal and Bratbak 1991), the indications strongly support the idea of a rapid turnover within the large viral population. It has been speculated (Bratbak et al. 1992)—and has also shown experimentally—that at least parts of the organic carbon (Bratbak et al. 1998) and the phosphorus (P) (Middelboe et al. 1996) released by viruses can be reused by bacteria. By defining the “microbial loop” as the loss of organic material by diverse processes from the particulate flux toward larger organisms in the food web and the reincorporation of this organic material via heterotrophic bacteria (Azam et al. 1983), one thus has a “viral loop” as a subset of the diverse release mechanisms of the microbial loop. As much as 25% of the primary production in the sea has been estimated to flow through this viral loop (Wilhelm and Suttle 1999). Energy is lost by respiration in a particularly short circuit when organic material from bacterial biomass flows via viral lysis to organic bacterial substrates and back into bacterial biomass. Such circular loops would also give a high rate of bacterial production relative to the rate of primary production (Strayer 1988), and an understanding of the mechanisms

that partition loss of bacterial production between protozoan predation and viral lysis is central to our understanding of the biogeochemical role of bacteria in the pelagic food web. This partitioning supposedly affects the flux of matter to larger plankton organisms that are capable of producing sinking material as well as the flux to trophic levels of commercial interest. Our understanding of the planktonic food web therefore seems very incomplete so long as we lack even a hypothesis for the underlying mechanisms controlling viral abundance.

Using an idealized model that assumes completely unselective protozoan predation on the bacteria and assuming the presence of viruses with high host specificity, Thingstad et al. (1997) argued that “reasonable” parameter values could allow on the order of 100 simultaneously dominant species of bacteria. Thingstad and Lignell (1997) used an idealized model of bacterial predation and competition to show that in the case of mineral nutrient bacterial growth rate, neither bacterial growth rate nor bacterial biomass would be affected by the introduction of an extra bacterial loss rate representing viral lysis. However, none of these analyses provides clues to the mechanisms controlling viral abundance and the magnitude of bacterial lysis. The most complete model available for virus-bacteria population dynamics seems to be the one analyzed by Levin et al. (1977). Since their focus leans toward bacteria-virus systems in chemostats rather than natural communities, it is, however, not immediately obvious from their analysis how viral abundance would be controlled in a larger food-web context. To approach this question, the somewhat analogous model used by Thingstad et al. (1997) and Thingstad and Lignell (1997) is analyzed here in more detail.

Model

The idealized situation we will explore (Fig. 1) consists of a set of m bacterial species with biomass B_i ($i = 1, \dots, m$), all of which are competing for the same limiting substrate with concentration N . To each bacterial species there is a corresponding virus with biomass V_i . There is also a

Acknowledgments

This work was financed through the EU MAST3 program, contract MAS3-CT97-0154, “MIDAS,” and a NORFA guest professorship. I thank Ian Dundas, Åke Hagstrøm, and Gunnar Bratbak for input and critical comments on this manuscript.

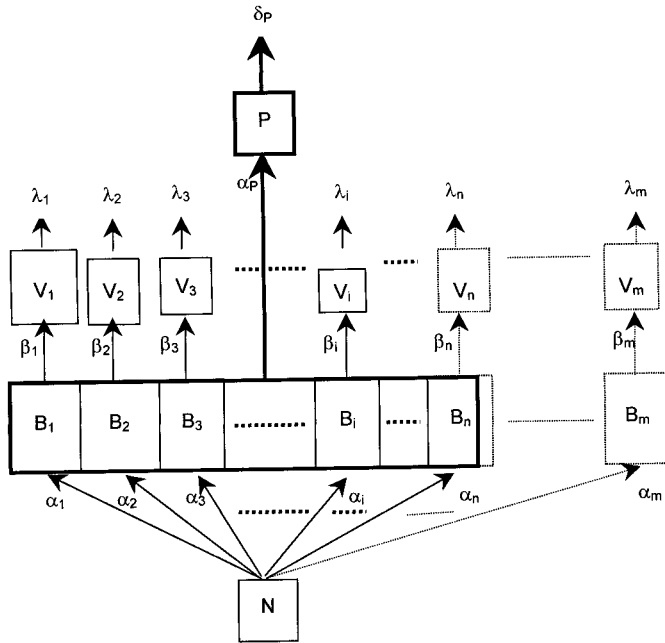


Fig. 1. Idealized structure analyzed. There are potentially m different bacterial host-lytic virus pairs, B_i - V_i , where the properties of the host-specific virus determine the steady-state biomass of the host. There is also a nonselective protozoan predator such that the properties of the protozoan determine the steady-state biomass of the total bacterial community. As explained in the text, there is room within the total community for $n - 1$ host-virus pairs, arranged in the order of sinking host affinity, α_i , for the common limiting substrate N . There is also room for a n th bacterial species that will not reach the biomass required for establishment of its virus and that will therefore only be subject to loss by protozoan predation. Viruses ($i > n - 1$) and hosts ($i > n$) not able to exist stably in the system are indicated by dotted contours.

protozoan predator with biomass P that captures all bacterial prey species with the same clearance rate, α_p . Virus i has an adsorption coefficient (analogous to clearance rate), β_i , for bacterial species i . Bacterial species i has a nutrient affinity (also analogous to clearance rate), α_i . A fraction Y_{bi} of the limiting nutrient is transferred to bacterial biomass, a fraction Y_{vi} of biomass in bacterial hosts is transferred to viruses, and a fraction Y_p of bacterial prey is transferred to the protozoan predator. Since we focus on steady-state relationships, we will disregard the latency time from infection to lysis of bacterial cells.

The total bacterial biomass B_T^* at steady state (superscripted * on variables is used to denote steady-state values) can be derived from the requirement that there must be enough prey to allow protozoa to grow as quickly as they are lost:

$$Y_p \alpha_p B_T^* P^* = \delta_p P^*, \quad (1)$$

where δ_p is the specific loss rate for protozoa. Solving for B_T^* gives the following:

$$B_T^* = \frac{\delta_p}{Y_p \alpha_p}. \quad (2)$$

An analogous argument for virus i gives the biomass of all

bacterial species for which there is a corresponding virus established in the system:

$$B_i^* = \frac{\lambda_i}{Y_{vi} \beta_i}, \quad (3)$$

where λ_i is the specific decay rate of virus i . Since the sum of biomasses for all coexisting bacterial species must equal B_T^* , we must have

$$\sum_{i=1}^n B_i^* = \sum_{i=1}^{n-1} \frac{\lambda_i}{Y_{vi} \beta_i} + B_n^* = B_T^*, \quad (4)$$

where n is the number of terms in the series on the left side that is needed to make the left side equal to the right side. Biomass B_n of the n th species is a special case, because, as we shall see below, there is no virus that is permanently established for this species. The rest of the $m-n$ bacterial species and their corresponding viruses will not be able to establish permanently in the system.

To understand more clearly what is happening, we will arrange the bacterial species according to decreasing nutrient affinity, α_i :

$$\alpha_1 > \alpha_2 > \dots > \alpha_n > \dots > \alpha_m \quad (5)$$

We can then illustrate the mechanisms regulating coexistence using the following hypothetical experiment: Assume that you have a system with only bacterial species No. 1 and the protozoan predator established. Bacterial species No. 1 can then grow up toward biomass B_T . If B_T is larger than $\lambda_1 / Y_{v1} \beta_1$, virus No. 1 can establish and bring the biomass of bacterial species No. 1 down to $\lambda_1 / Y_{v1} \beta_1$. The system can then be invaded by bacterial species No. 2, which can grow toward biomass $B_T - B_1$. If this biomass is great enough for virus No. 2 to establish ($> \lambda_2 / Y_{v2} \beta_2$), then the biomass of species No. 2 is reduced to $\lambda_2 / Y_{v2} \beta_2$. This reduction continues until species No. 1 and its virus are included. For species n , the biomass can only reach

$$B_n^* = B_T^* - \sum_{i=1}^{n-1} B_i^* \leq \frac{\lambda_n}{Y_{vn} \beta_n}, \quad (6)$$

before the size of the total bacterial community reaches the limit set by the protozoan predator. Host biomass will therefore not be sufficient to allow virus n to invade the system. Bacterial species $n + 1 \dots m$ will have a specific growth rate that is lower than the predation rate from protozoa, and it will therefore not be able to establish. With no hosts, the same result will of course be the case for virus $n + 1 \dots m$. The situation is illustrated in the food web of Fig. 1, which displays the solid contours of established members and the dotted contours of nonestablished members.

For any of the n coexisting species, the requirement that growth balances the sum of losses to viruses and protozoa gives the following equation:

$$Y_{Bi} \alpha_i N^* B_i^* = \beta_i B_i^* V_i^* + \alpha_p B_i^* P^*, \quad i = 1, \dots, n \quad (7)$$

Since B_i^* for all $i \leq n$, we can divide Eq. 7 by B_i^* to get

$$Y_{Bi} \alpha_i N^* = \beta_i V_i^* + \alpha_p P^*, \quad i = 1, \dots, n \quad (8)$$

In the special case of $i = n$, we have V_n^* , such that

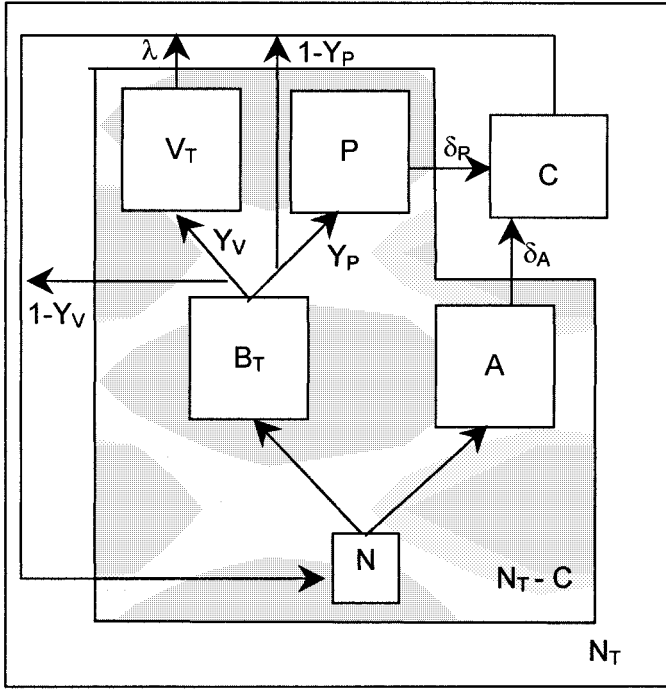


Fig. 2. Idealized food web with phytoplankton (A) competing with the bacterial community (B_T) for a common limiting mineral nutrient (N). Bacteria may be lost (via lysis) to viruses with an efficiency of transfer of the limiting element of Y_V or to protozoa (P) with an efficiency of transfer Y_P . The system inside the shaded area is assumed to be in internal steady state, with a total content of the limiting element of $N_T - C$. N_T is the total amount of the limiting element that is available, and C is the amount of the limiting element in a ciliate predator common to phytoplankton and bacterivorous protozoa.

$$P^* = Y_{Bn} \frac{\alpha_n}{\alpha_p} N^*. \quad (9)$$

Inserting Eq. 9 into Eq. 8 and solving for biomass of the i th viral species gives the following:

$$V_i^* = \frac{Y_{Bi} \alpha_i - Y_{Bn} \alpha_n}{\beta_i} N^*, \quad i = 1, \dots, n \quad (10)$$

For a given nutrient concentration N^* , a main determining factor for viral biomass is thus *the difference in nutrient affinity between the coexisting bacterial species*. The underlying mechanism is the steady-state condition that all bacterial species that grow faster than species n (as a result of their higher nutrient affinity) will also have to be lost at a correspondingly higher rate. In our model, this required increase in loss for bacteria with high nutrient affinity can only be accomplished by an increase in lysis. This increase can be caused either by an increased biomass of the virus or by a correspondingly lower adsorption coefficient, β_i , for the host-virus interaction.

Total biomass V_T^* of viruses is then

$$V_T^* = \sum_{i=1}^{n-1} V_i^* = N^* \sum_{i=1}^{n-1} \frac{Y_{Bi} \alpha_i - Y_{Bn} \alpha_n}{\beta_i} \quad (11)$$

This also gives us an expression for the viral : bacterial biomass ratio, f_{VB} ,

$$f_{VB} = \frac{V_T^*}{B_T^*} = \frac{N^*}{B_T^*} \sum_{i=1}^{n-1} \frac{Y_{Bi} \alpha_i - Y_{Bn} \alpha_n}{\beta_i}, \quad (12)$$

as well as the ratio f_{LP} between the bacterial loss by viral lysis and loss by protozoan predation:

$$f_{LP} = \frac{\sum_{i=1}^{n-1} \beta_i V_i^* B_i^*}{\alpha_p B_T^* P^*} = \sum_{i=1}^{n-1} \left(\frac{Y_{Bi} \alpha_i - Y_{Bn} \alpha_n}{Y_{Bn} \alpha_n} \right) \frac{B_i^*}{B_T^*}. \quad (13)$$

In order to obtain a simpler situation that is suitable for illustration of principles, we assume viral yields, viral adsorption coefficients, and viral decay rates to be equal for all species ($Y_{Vi} = Y_V$, $\beta_i = \beta$, and $\lambda_i = \lambda$ for all i), and we also assume all bacterial yields on the limiting substrate to be equal ($Y_{Bi} = Y_B$, $i = 1, \dots, n$) This gives us, from Eq. 13,

$$f_{LP} = \frac{1}{\alpha_n B_T^*} \frac{\lambda}{Y_V \beta} \sum_{i=1}^{n-1} (\alpha_i - \alpha_n). \quad (14)$$

Thus we have (by insertion in Eq. 6)

$$(n - 1) \frac{\lambda}{Y_V \beta} = B_T^* - B_n^* \quad \text{or} \quad \frac{\lambda}{Y_V \beta} = \frac{B_T^* - B_n^*}{n - 1} \approx \frac{B_T^*}{n - 1}. \quad (15)$$

The approximation is valid when $B_n^* \ll B_T^*$. Insertion into Eq. 14 gives the following:

$$f_{LP} \approx \frac{1}{n - 1} \frac{\sum_{i=1}^{n-1} (\alpha_i - \alpha_n)}{\alpha_n} \quad (16)$$

The partitioning of bacterial production between the loss to viral lysis and the loss to protozoan predation is thus approximately equal to the mean relative distance in affinity of the $n - 1$ infected species from the n th species (with the smallest affinity).

For V_T and f_{VB} , the expressions in Eqs. 11 and 12 contain the concentration N^* of the common limiting substrate. To move closer to an understanding of how the system changes with changing conditions, one therefore also needs a description for the mechanisms controlling N^* . To obtain this description, we add to our model a phytoplankton competitor (A) for mineral nutrients and we assume the algal cells to be too large to serve as prey for the bacterial predator (Fig. 2). Assuming steady state for the phytoplankton population gives, in analogy with Eq. 1,

$$Y_A \alpha_A N^* A^* = \delta_A A^*, \quad \text{or} \quad (17)$$

$$N^* = \frac{\delta_A}{Y_A \alpha_A}. \quad (18)$$

Insertion into Eqs. 11 and 12 gives the following:

$$V_T^* = \frac{Y_B}{Y_A} \frac{\delta_A}{\beta \alpha_A} \sum_{i=1}^{n-1} (\alpha_i - \alpha_n), \quad \text{and} \quad (19)$$

$$f_{VB} = \frac{Y_P}{Y_A} \frac{\alpha_P}{\alpha_A \beta} \frac{\delta_A}{\delta_P} \sum_{i=1}^{n-1} (\alpha_i - \alpha_n), \quad (20)$$

respectively. In a case in which loss rates of bacterivorous protozoa and phytoplankton are both being dominated by predation from a common, nonselective predator, as illustrated by the ciliate in Fig. 2, δ_A and δ_P become identical:

$$\delta_A = \delta_P = \alpha_C C, \quad (21)$$

where C is ciliate biomass and α_C is ciliate clearance rate. The loss rates δ_A and δ_P thus cancel each other out in the expression for the biomass ratio f_{VB} (Eq. 20):

$$f_{VB} = \frac{Y_P}{Y_A} \frac{\alpha_P}{\alpha_A \beta} \sum_{i=1}^{n-1} (\alpha_i - \alpha_n). \quad (22)$$

In Eqs. 19 and 20, n is also a variable. From insertion into Eq. 6, biomass of the n th bacterial species is given by the equation

$$B_n = \frac{\delta_P}{Y_P \alpha_P} - (n-1) \frac{\lambda}{Y_V \beta} \leq \frac{\lambda}{Y_V \beta}. \quad (23)$$

Each time δ_P increases by the critical amount $\lambda/Y_V \beta$, a new bacterial species is allowed to establish, so that the number of coexisting species increases from n to $n' = n + 1$. If, however, the difference between $\alpha_{Bn} - \alpha_{Bn'}$ is small, this increase in coexisting species will have little effect on the sums in the expressions above. In this case, f_{VB} becomes approximately constant (Eq. 22), whereas viral concentration will increase approximately proportionally to ciliate biomass (from Eqs. 20 and 21):

$$V_T^* = \left(\frac{Y_B}{Y_A} \frac{\alpha_C}{\beta \alpha_A} \sum_{i=1}^{n-1} (\alpha_i - \alpha_n) \right) C. \quad (24)$$

Combining the model with observed trends

Combining the model with observations gives some constraints on the model parameters. First, the result of Fuhrman and Noble (1995), which suggests an even partitioning of viral production between loss to viral lysis and to predation, is consistent with our model if (from Eq. 16)

$$\frac{1}{n-1} \frac{\sum_{i=1}^{n-1} (\alpha_i - \alpha_n)}{\alpha_n} \approx 1 \quad (25)$$

This means that for the model to be consistent with this observation, coexisting bacteria must be quite different. The mean distance in affinity of the $n-1$ infected species from the uninfected species must be of similar magnitude to the affinity of species n . However, later estimates seem to indicate a more variable partitioning, with viral lysis representing somewhere in the range of 10–50% of bacterial production (Fuhrman 1999; Wilhelm and Suttle 1999). This would allow for smaller differences between the coexisting bacteria.

Using Eq. 25, we can also simplify our expression for viral biomass (Eq. 24) and ratio between viral and bacterial biomass (Eq. 22) further to give the following:

$$V_T^* \approx \left(\frac{Y_B (n-1) \alpha_n \alpha_C}{Y_A \beta \alpha_A} \right) C, \quad \text{and} \quad (26)$$

$$f_{VB} = \frac{Y_P (n-1) \alpha_n \alpha_P}{Y_A \alpha_A \beta}, \quad (27)$$

respectively. The observation that the ratio of viral to bacterial abundance is roughly equal to 10 (Maranger and Bird 1995) can be stated as follows:

$$\frac{\rho_B}{\rho_V} f_{VB} \approx 10, \quad (28)$$

where ρ_B and ρ_V are the biomass of a bacterium and a virus, respectively. Our model will thus reproduce the observed trends if we choose parameters such that (combining Eqs. 28 and 27)

$$\frac{\rho_B}{\rho_V} \frac{Y_P}{Y_A} \frac{(n-1) \alpha_n \alpha_P}{\alpha_A \beta} \approx 10. \quad (29)$$

Simulation results

To illustrate the analysis, the differential equation analogues of Eqs. 1, 3, 7, and 17 and the parameter values given in Table 1 have been used to construct a numerical simulation model. The model was formulated in the Stella programming package running under Windows 95. A Runge–Kutta second-order procedure with time step 0.2 h was used. Phosphate has been assumed to be the common limiting nutrient, and all biomasses are calculated in phosphorus (P) units. The system has been initialized in the equilibrium calculated from the equations above, combined with the additional mass balance requirement for phytoplankton biomass A :

$$A^* = N_T - \left(\sum_{i=1}^n B_i^* + \sum_{i=1}^{n-1} V_i^* + N^* + P^* \right) \quad (30)$$

where N_T is the total P available to the system inside the shaded area of Fig. 2. Ciliate biomass, and thus phytoplankton and protozoan loss rates, were treated as constants in the simulation model. In each viral species, a lower limit of 10^{-4} $\mu\text{mol P m}^{-3}$ has also been assumed to avoid excessive time for reestablishment of viral populations. With the parameters chosen (Table 1), the initial steady state is locally stable both at the level of the total bacterial and viral communities (Fig. 3A) and at the level of the individual host–virus pairs (Fig. 3C,D). Note that with these parameters, the five infected bacterial species all have the same biomass, whereas the uninfected bacterial species No. 6 has a lower biomass (Fig. 3C). Biomass of the viruses, however, decreases in the sequence 1–5 (Fig. 3D), corresponding to the decrease in the nutrient affinity of the virus' host. To illustrate the way the model functions, bacterial species No. 7, which was initially unable to invade the system, is allowed to “mutate” at time = 100 h by changing α_7 from 0.065 to 0.11 $\text{m}^3 \mu\text{mol P}^{-1}$

Table 1. Symbols, parameter values, and initial steady-state values of variables.

Parameters							
Symbol	Value					Unit	Meaning
α_A	0.3					$\text{m}^3 \mu\text{mol P}^{-1}\text{h}^{-1}$	Algal-specific affinity for phosphate
α_i	0.21	0.18	0.15	0.12	0.09	$\text{m}^3 \mu\text{mol P}^{-1}\text{h}^{-1}$	Bacterial-specific affinity for phosphate, species $i = 1..10$
$i = 1..10$	0.07	0.065	0.06	0.055	0.050	$\text{m}^3 \mu\text{mol P}^{-1}\text{h}^{-1}$	Protozoan-specific clearance rate for bacteria
α_p	0.008					$\text{m}^3 \mu\text{mol P}^{-1}\text{h}^{-1}$	Viral-specific adsorption constants $i = 1..10$
β_i	0.8					$\text{m}^3 \mu\text{mol P}^{-1}\text{h}^{-1}$	Algal-specific loss rate
δ_A	0.033					h^{-1}	Protozoan-specific loss rate
δ_p	0.033					h^{-1}	Viral-specific decay rate, $i = 1..10$
λ_i	0.2					h^{-1}	Fraction of P in bacterial prey transferred to predator biomass
Y_p	0.3					Dimensionless	Fraction of P in bacterial host transferred to viruses
Y_v	0.1					Dimensionless	Ratio of bacterial to viral P content
$\rho_B : \rho_V$	300					Dimensionless	Total P available for sharing between food-web components.
P_i	100					$\mu\text{mol P m}^{-3}$	
Variables							
Symbol	Computed equilibrium values using parameter values above					Unit	Meaning
n	6 (from Eq. 6)					Dimensionless	No. of coexisting species
f_{LP}	1.04					Dimensionless	Ratio of lysis to predation
f_{VB}	12.0					Dimensionless	Ratio of viral to bacterial abundance
B_i	2.5	2.5	2.5	2.5	2.5	$\mu\text{mol P m}^{-3}$ or $10^8 \text{ cells L}^{-1}$	Bacterial biomass or abundance
$i = 1..10$	1.25	10^{-4}	10^{-4}	10^{-4}	10^{-4}	$\mu\text{mol P m}^{-3}$	Viral biomass
V_i	0.19	0.15	0.11	0.069	0.028	$\mu\text{mol P m}^{-3}$	Abundance
$i = 1..10$	10^{-4}	10^{-4}	10^{-4}	10^{-4}	10^{-4}	$10^9 \text{ viruses L}^{-1}$	
V_i	5.8	4.5	3.3	2.1	0.8	$10^9 \text{ viruses L}^{-1}$	
$i = 1..10$	3×10^{-3}	3×10^{-3}	3×10^{-3}	3×10^{-3}	3×10^{-3}	$\mu\text{mol P m}^{-3}$	Phytoplankton biomass
A	75					$\mu\text{mol P m}^{-3}$	Protozoan biomass
P	9.6					$\mu\text{mol P m}^{-3}$	Free orthophosphate
N	1.1					$\mu\text{mol P m}^{-3}$	

h^{-1} , thereby changing its relative position, in the sequence of affinities, from 7 to 5. Note how bacterial species No. 6 and virus species No. 5 both disappear after the mutation, to be replaced by bacterial species No. 7 and its virus. The transient response to this disturbance is, however, quite long-lived (Fig. 3). Since the “mutation” of bacterial species No. 7 leads to an exchange of bacterial species No. 6 with bacterial species No. 5 as the established species with the lowest affinity (α_n in the equations), the expression for the partitioning of bacterial production in Eq. 16 will be reduced, as will the virus:bacteria ratio (Eq. 20) (Fig. 3B).

Discussion

The key principle for control of viral abundance in the model analyzed here is that viruses act as a balancing factor, by which bacterial species with different growth rates (but which are subject to a similar loss to predation) can all coexist in steady state. If all host-virus systems have similar adsorption coefficients (β_i), viruses with fast-growing hosts

(high α_i) are predicted to be the most abundant (Fig. 3D). The model thus indicates the presence of a reciprocal controlling principle between viruses, bacterial diversity, and the biogeochemical fate of bacterial production. Although the idea of viral control of the number of dominant bacterial species is not new (Bergh et al. 1989; Thingstad and Lignell 1997; Thingstad et al. 1997), the idea that bacterial diversity (in the sense of *differences* between the coexisting species) controls viral abundance seems not to have been similarly acknowledged. Likewise, the common idea that high diversity leads to numerous pathways for biogeochemical transport of matter and energy through the food web is intuitively acceptable. The idea that the magnitude of the differences between coexisting bacterial species influences the partitioning between major alternative loss routes for bacterial production is, however, not so immediately obvious.

In the simple version analyzed here, the model contains no linkages in the form of trade-offs between parameters. The consequence is that there are interesting evolutionary questions that cannot be answered without additional as-

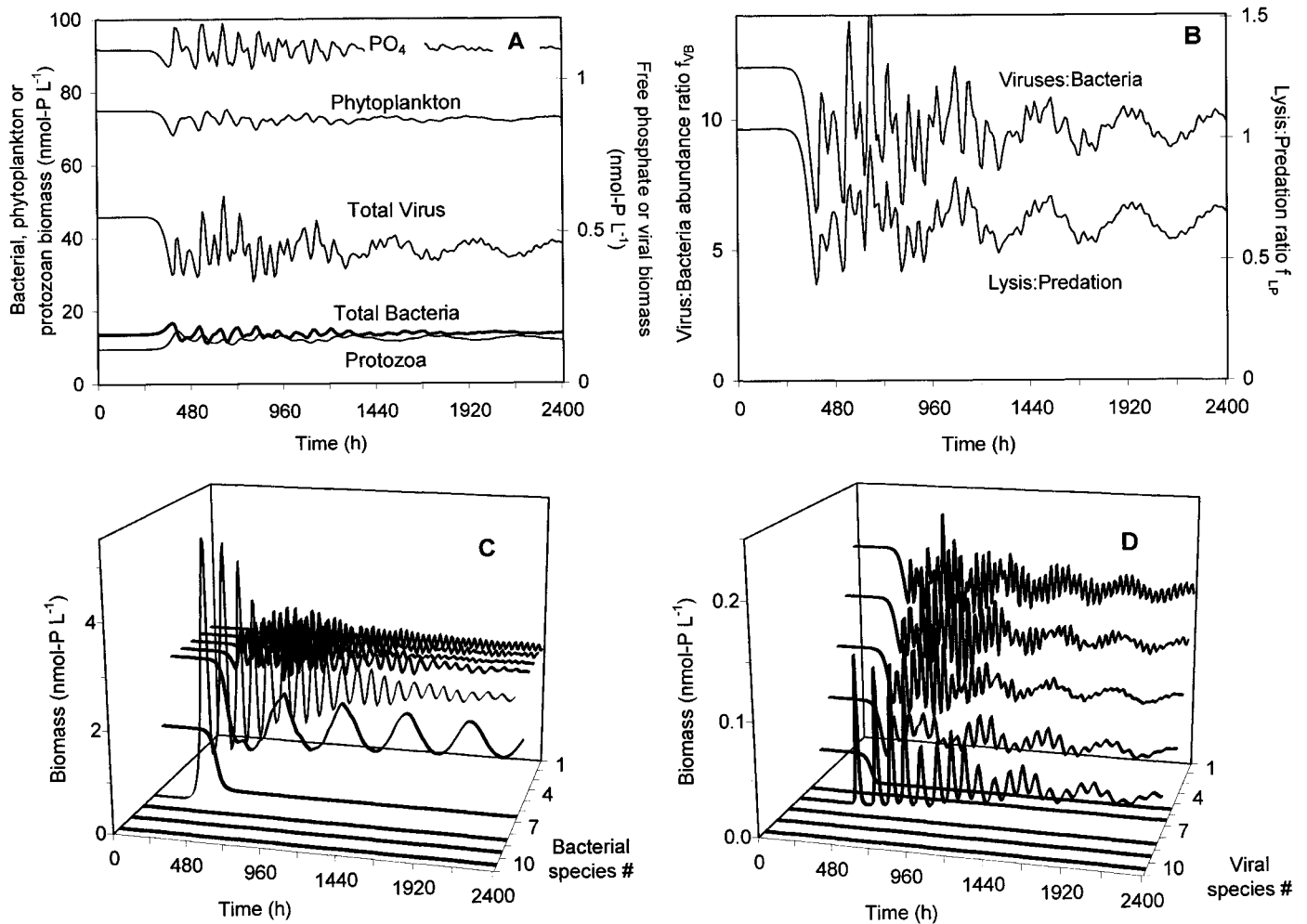


Fig. 3. Simulation study of the model in Figs. 1 and 2, using the parameters in Table 1. (A) Biomass in phosphorus (P) units of total bacteria and total viruses, phytoplankton, bacterivorous protozoa, and free phosphate. (B) Virus : bacteria abundance ratio and lysis : predation loss-rate ratio. (C) Biomass of individual bacterial species. (D) Biomass of individual viral species. The simulation was started in the theoretical steady state discussed in the text. At time = 100 h, the affinity α_7 of bacterial species No. 7 was changed from 0.065 to 0.11. Since following the "mutation" $\alpha_7 > \alpha_5 > \alpha_6$, bacterial species No. 7 replaced bacterial species No. 6, and virus No. 7 replaced virus No. 5. Further discussion in the text.

sumptions. As illustrated by the simulated mutation experiment, a bacterium that can mutate to get an affinity constant α_i that is larger than the present minimum value α_n for established species will always be able to invade the bacterial community. Species n is then lost. In such a "simple" world, one would thus expect the selection to favor bacteria that evolve toward higher α . The result would seem to be that all coexisting species should cluster just below the highest possible affinity, where they are limited in an upward direction by the physics of diffusion and the smallest size that is biologically attainable. The expected result of evolution would then be a low relative distance between bacterial affinities, and hence, both a small virus : bacteria ratio (Eq. 12) and a small fraction of bacterial loss would be caused by viruses (Eq. 13). Since this prediction appears to be in contradiction with present observations, there must be additional selective forces that spread the affinity constants. Trade-offs between susceptibility to virus and nutrient uptake capabil-

ities are likely to occur. Porins for maltose transport serve as attachment sites for λ -phages (see review by Nikado and Vaara [1987]), and the porin for nucleoside transport seem to provide the attachment site for phage T6 (see review by Schwartz [1987]). Modification of the porins may thus reduce the adsorption of viruses but will likely reduce the nutrient affinity at the same time. In the terminology of our model, this would mean that mutation toward higher nutrient affinity α_i carries a price in the form of a linked increase in the viral adsorption coefficient β_i . Since growth rate $\mu_i = \alpha_i N$ is proportional to affinity α_i , and because biomass is proportional to the inverse of adsorption coefficient β_i (Eq. 2), the steady-state biomass and growth rate distributions for the bacterial host species would in this case display opposite trends. Bacterial hosts with high α and β would have high growth rates but low biomass, whereas species with low α and β would have low growth rates but high biomass. Since bacterial production is the product $\mu_i B_i$, bacterial production

at steady state will be proportional to the ratio α_i/β_i . If the α_i and β_i are proportional, production will therefore be the same for all infected species. If, however, a mutation leads to a proportionally larger decrease in β (larger resistance to viral infection) than in α (loss of nutrient affinity), such mutations will increase production. If selection pressure favors species with a high total rate of reproduction (i.e., a high production), one would in the latter case get a selective force toward lower α for all established species. All unestablished species would, however, still need to mutate toward higher α in order to invade the system, and the two opposite trends may possibly lead to a spread in α values. Obviously, a more sophisticated model is needed in order to explain why the mean relative distance in bacterial affinities should evolve toward values as large as 1, as is indicated by Eq. 25.

Another relevant observation in this discussion is Waterbury and Valois's (1993) finding that they could isolate a diverse and abundant population of *Synechococcus* viruses but that most of the cells in the natural *Synechococcus* populations were resistant to these viruses. To allow for coexistence, our simple model needs some kind of mechanism that specifically increases the loss of the most efficient competitor. Coexistence of completely virus-resistant species in a homogeneous environment therefore would require an alternative specific loss mechanism, such as, for example, different α_p for different *Synechococcus* species.

As noted also by Levin et al. (1977), it seems quite easy to find parameter values that makes the steady state of these systems locally stable. Experimental evidence seems to indicate that population shifts in bacteria occur on seasonal scales (Rehnstam et al. 1993; Höfle and Brettar 1995; Murray et al. 1998; Höfle et al. 1999), whereas it may be too early to conclude on the occurrence of oscillations on the daily scales expected if they are driven by the internal predator-prey interaction of viruses and bacteria. By linearization of the Lotka-Volterra equations for the simple predator-prey system (with a fixed prey growth rate, μ , and a fixed predator death rate, δ), one can show that the frequency of small-amplitude oscillations should be approximately $\sqrt{\mu\delta}$. In our model, we would expect a coupling between the oscillators formed both by the outer predator-prey system of the total bacterial community and by the protozoa and the multiple inner systems of hosts and viruses. In our simulated mutation experiment, we can see the effect of this coupling. The damped oscillations following the perturbation are dominated by the higher frequency modes for the high-affinity species, whereas for the low-affinity species, the dominating mode is of longer frequency (Fig. 3C,D). For a locally unstable equilibrium, one would expect these coupled oscillations to at least appear to be chaotic. Our model does not include the complications of a latency time between viral infection and bacterial lysis. Time delays would generally be expected to destabilize otherwise stable dynamic equilibria (e.g., Thingstad and Langeland 1974; Levin et al. 1977). There are, however, also mechanisms that would stabilize such oscillations. A highly relevant possibility is lysogeny (Jiang and Paul 1996), which functions in this context as a potential refuge, thereby preventing extreme reductions in viral abundance. In their experiments with host-virus systems in chemostats, Levin et al. (1977) noted the inability

of their model to predict the stability properties of the experimental system. Beyond the demonstrated possibility of creating stable equilibria, the stability properties of the equilibrium should not be regarded as a robust feature of the model.

To limit the simulation model to a practical size, we used only 10 bacterial populations and we chose parameters for lysis and predation that allowed six of these populations to coexist in steady state. The total number of species present is probably much higher, as reflected in the old paradigm that "everything is everywhere." Most of these species, however, may be present only in very low numbers. The total number of species is, however, of less relevance to the principles discussed here. More interesting is the number of simultaneously dominant species. Thingstad et al. (1997) suggested that by using "reasonable" parameter values for lysis and predation, one could theoretically expect up to 100 simultaneously dominant species in the marine pelagic. With a total bacterial abundance of around 10^9 L⁻¹, this corresponds to an average abundance for each dominant species of around 10^7 L⁻¹. Interestingly, this is the level found for the hosts in the experimental chemostat host-virus systems studied by Levin et al. (1977). The recent studies using molecular techniques based on 5S (Höfle and Brettar 1995) or 16S ribonucleic acid (Øvreås et al. 1997) seem to indicate a lower number of simultaneously dominant bacterial species in natural aquatic environments—a number more on the order of 5–15.

In the real world, the network of selective and unselective predation is probably quite complex, and changes in the predatory community are known to have effects on the bacterial species composition (Simek and Chrzanowski 1992; Pernthaler et al. 1996; Simek et al. 1999). To what extent the simplifying assumptions have to be relaxed before real systems can be represented is therefore presently unknown.

The model used here for bacteria and their viruses can be applied directly to other functional groups in the food web of Fig. 2. An obvious example would be phytoplankton, which by now is well known to be subject to viral attack (Cottrell and Suttle 1995; Bratbak et al. 1998; Brussaard et al. 1999).

Discussions of coexistence based on the traditional concept that there should be as many resources as there are stably coexisting species become awkward in complex predator-prey networks with competition like that indicated in Figs. 1 and 2. This is primarily because of the difficulties, in such cases, in defining "resources" in a satisfactory manner. A simpler and intuitively more attractive principle that grasps most of the underlying principles in the analysis made here is that equilibrium diversity in these networks is maintained by mechanisms that are selectively "killing the winner." Coexistence among bacteria is ensured by host-specific viruses that prevent the best bacterial competitors from building up a high biomass, and coexistence of mineral nutrient-limited phytoplankton and bacteria is ensured by size-selective grazers that prevent the bacteria from immobilizing all of the limiting nutrient in bacterial biomass.

This model gives a kind of hierarchical theory for top-down control of diversity in the microbial part of the food web. At the top level there is the total content of the limiting

element, setting the limit for total biomass. Then there is size-selective predation that allows for distribution of the limiting element into different functional groups, as in Fig. 2, and finally there is viral host specificity, which allows for further distribution into different species inside each functional group, as in Fig. 1. Note that all arguments used for coexistence in this model are based on steady-state assumptions. Mechanisms such as spatial and temporal variability would, at least for intermediate disturbances (Sommer 1995), be expected to increase diversity even further. With present evidence suggesting a fairly low number of dominant bacterial species in aquatic environments, it is then no longer obvious that the problem is how a high diversity can be maintained in an apparently stable environment with a (presumably) low number of limiting substrates (Hutchinson 1961). Maybe Hutchinson's paradox should be reversed: Why are there so few dominating species when simple steady-state models can predict so many?

References

- AZAM, F., T. FENCHEL, J. G. FIELD, J. S. GRAY, L. A. MEYER-REIL, AND T. F. THINGSTAD. 1983. The ecological role of water-column microbes in the sea. *Mar. Ecol. Prog. Ser.* **10**: 257–263.
- BERGH, Ø., K. Y. BØRSHEIM, G. BRATBAK, AND M. HELDAL. 1989. High abundance of viruses found in aquatic environments. *Nature* **340**: 467–468.
- BRATBAK, G., M. HELDAL, T. F. THINGSTAD, B. RIEMANN, AND O. H. HASLUND. 1992. Incorporation of viruses into the budget of microbial C-transfer. A first approach. *Mar. Ecol. Prog. Ser.* **83**: 273–280.
- , A. JACOBSEN, AND M. HELDAL. 1998. Viral lysis of *Phaeocystis pouchetii* and bacterial secondary production. *Aquat. Microb. Ecol.* **16**: 11–16.
- , T. F. THINGSTAD, AND M. HELDAL. 1994. Viruses and the microbial loop. *Microb. Ecol.* **238**: 209–221.
- BRUSSAARD, C., R. THYRHAUG, D. MARIE, AND G. BRATBAK. 1999. Flow cytometric analyses of viral infection in two marine phytoplankton species, *Micromonas pusilla* (Prasinophyceae) and *Phaeocystis pouchetii* (Prymnesiophyceae). *J. Phycol.* **35**: 941–948.
- COTTRELL, M. T., AND C. A. SUTTLE. 1995. Dynamics of a lytic virus infecting the photosynthetic marine picoflagellate *Micromonas pusilla*. *Limnol. Oceanogr.* **40**: 730–739.
- FUHRMAN, J. 1999. Marine viruses and their biogeochemical and ecological effects. *Nature* **399**: 541–548.
- FUHRMAN, J. A., AND R. T. NOBLE. 1995. Viruses and protists cause similar bacterial mortality in coastal seawater. *Limnol. Oceanogr.* **40**: 1236–1242.
- HELDAL, M., AND G. BRATBAK. 1991. Production and decay of viruses in aquatic environments. *Mar. Ecol. Prog. Ser.* **72**: 205–212.
- HÖFLE, M., AND I. BRETTAR. 1995. Taxonomic diversity and metabolic activity of microbial communities in the water column of the central Baltic Sea. *Limnol. Oceanogr.* **40**: 868–874.
- , H. HAAS, AND K. DOMINIK. 1999. Seasonal dynamics of bacterioplankton community structure in a eutrophic lake as determined by 5S rRNA analysis. *Appl. Environ. Microbiol.* **65**: 3164–3174.
- HUTCHINSON, G. E. 1961. The paradox of the plankton. *Am. Nat.* **95**: 137–145.
- JIANG, S., AND J. PAUL. 1996. Occurrence of lysogenic bacteria in marine microbial communities as determined by prophage induction. *Mar. Ecol. Prog. Ser.* **142**: 27–38.
- LEVIN, B. R., F. M. STEWART, AND L. CHAO. 1977. Resource-limited growth, competition, and predation: A model and experimental studies with bacteria and bacteriophage. *Am. Nat.* **111**: 3–24.
- MARANGER, R., AND D. BIRD. 1995. Viral abundance in aquatic systems—a comparison between marine and fresh-waters. *Mar. Ecol. Prog. Ser.* **121**: 217–226.
- MIDDELBOE, M., N. O. G. JORGENSEN, AND N. KROER. 1996. Effects of viruses on nutrient turnover and growth efficiency of non-infected marine bacterioplankton. *Appl. Environ. Microbiol.* **62**: 1991–1997.
- MURRAY, A., C. PRESTON, R. MASSANA, L. TAYLOR, A. BLAKIS, K. WU, AND E. DELONG. 1998. Seasonal and spatial variability of bacterial and archaeal assemblages in the coastal waters near Anvers Island, Antarctica. *Appl. Environ. Microbiol.* **64**: 2585–2595.
- NIKAIDO, H., AND M. VAARA. 1987. Outer membrane, p. 7–23. *In* J. Ingraham, K. Low, B. Magasanik, M. Schaechter, and H. Umbarger [eds.], *Escherichia coli* and *Salmonella typhimurium*. Cellular and molecular biology, American Society for Microbiology.
- NOBLE, R., AND J. FUHRMAN. 1998. Use of SYBR Green I for rapid epifluorescence counts of marine viruses and bacteria. *Aquat. Microb. Ecol.* **14**: 113–118.
- ØVREÅS, L., L. FORNEY, F. DAAE, AND V. TORSVIK. 1997. Distribution of bacterioplankton in meromictic Lake Saelenvannet, as determined by denaturing gradient gel electrophoresis of PCR-amplified gene fragments coding for 16S rRNA. *Appl. Environ. Microbiol.* **63**: 3367–3373.
- PERNTHALER, J., B. SATTLER, K. SIMEK, A. SCHWARZENBACHER, AND R. PSENNER. 1996. Top-down effects on the size–biomass distribution of a freshwater bacterioplankton community. *Aquat. Microb. Ecol.* **10**: 255–263.
- PROCTOR, L. M., AND J. A. FUHRMAN. 1990. Viral mortality of marine bacteria and cyanobacteria. *Nature (Lond.)* **343**: 60–62.
- REHNSTAM, A.-S., S. BÄCKMAN, D. C. SMITH, F. AZAM, AND Å. HAGSTRØM. 1993. Blooms of sequence-specific culturable bacteria in the sea. *FEMS Microbiol. Ecol.* **102**: 161–166.
- SCHWARTZ, M. 1987. The maltose regulon, p. 1482–1502. *In* J. Ingraham, K. Low, B. Magasanik, M. Schaechter, and H. Umbarger, [eds.], *Escherichia coli* and *Salmonella typhimurium*. Cellular and molecular biology. American Society for Microbiology.
- SIMEK, K., AND T. CHRZANOWSKI. 1992. Direct and indirect evidence of size-selective grazing on pelagic bacteria by freshwater nanoflagellates. *Appl. Environ. Microbiol.* **58**: 3715–3720.
- , P. KOJECKÁ, J. NEDOMA, P. HARTMAN, J. VRBA, AND J. DOLAN. 1999. Shifts in bacterial community composition associated with different microzooplankton size fractions in a eutrophic reservoir. *Limnol. Oceanogr.* **44**: 1634–1644.
- SOMMER, U. 1995. An experimental test of the intermediate disturbance hypothesis using cultures of marine phytoplankton. *Limnol. Oceanogr.* **40**: 1271–1277.
- STRAYER, D. 1988. On the limits to secondary production. *Limnol. Oceanogr.* **33**: 1217–1220.
- THINGSTAD, T. F., G. BRATBAK, M. HELDAL, AND I. DUNDAS. 1997. Trophic interactions controlling the diversity in pelagic microbial food webs. Proceedings from the International Symposium in Microbial Ecology (ISME-7). Santos, Brazil 27 August–1 September, 1995. M. T. Martins, M. I. Z. Sato, J. M. Tiedje, et al., Brazilian Society for Microbiology/ICOME International Committee on Microbial Ecology.
- , AND T. LANGELAND. 1974. Dynamics of chemostat culture,

- the effect of a delay in cell response. *J. Theor. Biol.* **48**: 149–159.
- , AND R. LIGNELL. 1997. A theoretical approach to the question of how trophic interactions control carbon demand, growth rate, abundance, and diversity. *Aquat. Microb. Ecol.* **13**: 19–27.
- WATERBURY, J., AND F. VALOIS. 1993. Resistance to cooccurring phages enables marine *synechococcus* communities to coexist with cyanophages abundant in seawater. *Appl. Environ. Microbiol.* **10**: 3393–3399.
- WILHELM, S., AND C. SUTTLE. 1999. Viruses and nutrient cycles in the sea. *Bioscience* **49**: 781–788.

Received: 12 January 2000

Accepted: 17 May 2000

Amended: 7 June 2000